Microstructures of a Cylinder-Forming Diblock Copolymer under Spherical Confinement

Peng Chen[†,‡] **and Haojun Liang***[,†,‡]

Hefei National Laboratory for Physical Sciences at Microscale and Department of Polymer Science and Engineering, University of Science and Technology of China, Hefei, Anhui, 230026, People's Republic of China

An-Chang Shi*

Department of Physics and Astronomy, McMaster University, Hamilton, Ontario L8S 4M1, Canada

Received February 28, 2008; Revised Manuscript Received September 13, 2008

ABSTRACT: Self-assembly of cylinder-forming diblock copolymers under spherical confinement is studied using real-space self-consistent field theory calculations (SCFT). Various microstructures are found at different confinement dimensions and surface fields. Most of these microstructures are center-symmetric and they could not be formed in bulk or under planar and cylindrical confinements. It is also observed that the interactions between the confinement surface and the polymers have a large effect on the self-assembly. When the spherical confinement's surface attracts the short blocks, the self-assembled structures become similar to those under a neutral surface field. On the other hand, when the spherical confinement's surface attracts the long blocks, the equilibrium structures become different from those under a neutral surface field.

Introduction

Nanoscale structures assembled from block copolymers have gained much attention owing to their potential application in the production of polymeric nanostructured materials.[1−5] In the effort to develop methods to control structures, a number of theoretical and experimental studies have focused on the self-assembly of block copolymers under confined environments. Confined self-assembly provides a novel method of fabricating ordered structures which are not readily available in bulk systems.[6−10] Previous studies mostly focused on the case of one-dimensional (1-D) planar confinement, in which frustration on the polymeric microstructures leads to different orientations, as well as transitions from the bulk structures to other unusual structures.[10−18] Recently, experimental and theoretical studies have been broadened to include the case of two-dimensional (2-D) confinement for block copolymers.[19−24] Wu et al. examined silica−copolymer composite assembly upon 2-D cylindrical confinement. They realized that the system would employ a coiling strategy to pack in a limited cylindrical space.[25] Russell's group studied symmetric (lamella-forming) and asymmetric (cylinder-forming) polystyrene-*b*-polybutadiene diblock copolymers under 2-D cylindrical confinement. They found that the structures transit from lamellae to a stacked-disk or toroidal-type structure for a symmetric diblock copolymer, and helix structures were formed from cylinders for an asymmetric diblock copolymer.[26,27] The lamellae and helix structures are reproduced by theoretical studies.[23,28−32] Sevink et al. elaborately reproduced the toroidal-type structure using the dynamic density functional theory (DDFT) method.[33] Theoretical studies have predicted further complex microstructures under 2-D cylindrical confinement. The confinement dimension d/L, that is, the ratio of confinement diameter d versus polymer period in the bulk L, is found to control the structure transition in the confinement-induced block copolymer self-assembly.[28,29,34]

Relatively fewer studies have been conducted on the self-assembly of block copolymers under three-dimensional (3-D) spherical confinement. Thomas and co-workers examined the self-assembly of block copolymers or copolymer and homopolymer blends in microdroplets. For the bulk lamella-forming system, concentric shell structures in the droplet were observed.[35] Concentric structure was observed in our Monte Carlo simulation.[6] Arsenault et al. observed similar structures in their study of polystyrene-*b*-polyferrocenylethylmethysilane self-assembly in silica spherical cavities.[36] For the bulk gyroid-forming system, Thomas et al. observed a honeycomb-like structure in the droplet, suggesting a curvature-driven gyroid to perforated-layer transition. For the bulk cylinder-forming system, it seemed to pack into curved concentric arrays in the droplets.[35] Fraaije et al. studied the polymer surfactant droplet in weakly selective solvent using self-consistent field theory (SCFT) calculations. Their system is similar to a soft spherical confinement case, but the solvent could be taken up or released by the droplet. A series of unique structures were found under the condition of different block ratios in their study.[37] All these previous studies predicted a rich variety of novel microstructures under 3-D spherical confinements. Simultaneous with the completion of our work, there were two interesting research papers published. In a Monte Carlo study, Yu et al. systemically examined the self-assembly of symmetric diblock copolymers confined in spherical nanopores.[38] They identified a sequence of structures, from perpendicular lamellae to helices and/or embedded structures and concentric-spherical lamellae with surface preference increasing under this 3-D confinement. Feng et al. studied symmetric and asymmetric diblock copolymers in nanospheres using the dissipative particle dynamics approach.[39] They found in some cases that polymer in a nanosphere can be utilized to mimic the polymer surfactant.

Polymer chains may be under more severe frustrations in 3-D confinements as the constraint imposed by the environment cannot be released by reorienting the structure along the unconfined directions, in contrast to the 1-D and 2-D confinement cases. On the other hand, surface fields are imposed in all directions under 3-D confinement, causing the polymer system to undergo different surface reconstructions in comparison with the systems under 1-D and 2-D confinement. Therefore, it is desirable to understand the manner in which copolymers would respond under 3-D confinement. In this research, a systematic

* To whom correspondence should be addressed. E-mail: hjliang@ustc.edu.cn (H.L.); shi@mcmaster.ca (A.-C.S.).
† Hefei National Laboratory for Physical Sciences at Microscale.
‡ Department of Polymer Science and Engineering.

10.1021/ma800443h CCC: $40.75
Published on Web 10/29/2008

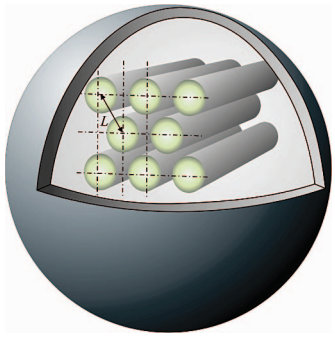

Figure 1. Schematic illustration of 3-D spherical confinement. L is polymer repeat period of bulk cylinders.

study on self-assembled microstructures from a bulk cylinder-forming diblock copolymer under spherical confinement using SCFT calculation is presented. The schematic illustration of 3-D spherical confinement is shown in Figure 1, wherein the cylinder-forming diblock copolymer is confined in a spherical cavity. The effects of surface field and confinement space diameter on the diblock copolymer self-assembly are considered. The self-assembled structures and phase behavior of the diblock copolymer under 3-D spherical confinement are discovered to be far more complex than those under the 1-D and 2-D confined environments.

Theory

The self-consistent field theory (SCFT) is a successful theoretical method for investigating block copolymer phase diagrams. The real-space approach scheme introduced by Fredrickson and Drolet[40−42] in solving self-consistent equations is employed in this study.

An incompressible melt of diblock copolymer with a degree of polymerization N is chosen for this research. The copolymer chain is composed of two blocks (A- and B-blocks), and the volume fraction of the A-block is specified by f_A ($0 < f_A < 1$). A Flory−Huggins interaction parameter χ_{AB} is used to characterize the repulsion between the A- and B-blocks. Periodic boundary conditions are imposed in all three dimensions to obtain the bulk structure of the diblock copolymers. For the 3-D spherical confinement case, there is no periodic boundary condition in any direction in the calculation. Under the confinement case, the diblock copolymer is confined in a spherical cavity of diameter d and volume V. The SCFT free energy per chain in the unit of k_BT has the form

$$F = -\ln\left(\frac{Q}{V}\right) + \frac{1}{V}\int \mathrm{d}r\,[\chi_{AB}N\phi_A\phi_B - \omega_A\phi_A - \omega_B\phi_B + h_{SA}\phi_A + h_{SB}\phi_B - P(\phi_0 - \phi_A - \phi_B)] \quad (1)$$

where ϕ_A and ϕ_B are the monomer densities and $\phi_0 = \phi_A + \phi_B$ is the total monomer density. The single-chain partition function $Q = \int \mathrm{d}r\ q(r,1)$ is the partition function of a single diblock copolymer chain in the mean fields, ω_A and ω_B, which are in turn produced by the surrounding chains. The end-segment distribution function, $q(r,s)$, is the probability that a chain segment of contour length s containing a free chain end has its "connected end" located at r. The function $q(r,s)$ and its conjugate $q'(r,s)$ satisfy the following modified diffusion equations:

$$\frac{\partial}{\partial s}q(r,s) = R_g^2\nabla^2 q(r,s) - N\omega q(r,s) \quad (2)$$

$$-\frac{\partial}{\partial s}q'(r,s) = R_g^2\nabla^2 q'(r,s) - N\omega q'(r,s) \quad (3)$$

with the initial conditions $q(r,0) = 1$ and $q'(r,1) = 1$. In these expression, R_g is the gyration radius for an ideal Gaussian chain. For $0 \le s \le f_A$, $\omega = \omega_A$, and $f_A < s \le 1$, $\omega = \omega_B$. The Crank−Nicholson scheme for solving these modified diffusion equations is used.

In eq 1, h_{SA} and h_{SB} represent the surface field that the inner surface of the confinement acts on A- and B-block, respectively. P is a Lagrange multiplier (as a pressure) used to ensure the incompressibility condition. Minimizing the free energy with respect to the densities and mean fields leads to the following SCFT equations:

$$\omega_A(r) = \chi_{AB}(\phi_B(r) - f_B) + h_{SA}(r) + P(r) \quad (4)$$

$$\omega_B(r) = \chi_{AB}(\phi_A(r) - f_A) + h_{SB}(r) + P(r) \quad (5)$$

$$\phi_A(r) = \frac{V}{Q}\int_0^{f_A} \mathrm{d}s\ q(r,s)\ q'(r,s) \quad (6)$$

$$\phi_B(r) = \frac{V}{Q}\int_{f_A}^{1} \mathrm{d}s\ q(r,s)\ q'(r,s) \quad (7)$$

These equations can be solved self-consistently.

The surface−polymer interaction is assumed to be short-ranged and is represented by the following contact interactions:

$$h_{SA(B)} = \begin{cases} H_{A(B)} & \text{on the lattices next to the surfaces} \\ 0 & \text{bulk} \end{cases} \quad (8)$$

Here, $H_{A(B)}$ is the strength of the surface field, which has the same unit as the Flory−Huggins interaction parameter χ_{AB}. To present the fact that polymer densities should approach zero at the confinement surface, the incompressibility condition is modified as $\phi_A(r) + \phi_B(r) = \phi_0(r)$, where $\phi_0(r)$ is set at 0.5 on the lattices next to the surfaces and 1 everywhere else. On the surface sites of the confinement, the end-segment distribution functions and polymer densities are set to zero.

Five types of confinement surfaces are considered: (a) neutral surfaces, wherein the surface has no preference for any block ($H_A = 0$ and $H_B = 0$, or in short $H = 0$); (b) weak A-attractive surface, wherein the confinement surface weakly attracts A-blocks ($H_A = -7$ and $H_B = 0$); (c) strong A-attractive surface, wherein the confinement surface strongly attracts A-blocks ($H_A = -14$ and $H_B = 0$); (d) weak B-attractive surface, wherein the confinement surface weakly attracts B-blocks ($H_A = 0$ and $H_B = -7$); and (e) strong B-attractive surface, wherein the confinement surface strongly attracts B-blocks ($H_A = 0$ and $H_B = -14$).

In these calculations, chain contour length is divided into 200 segments and the lattice constant is taken as $0.2R_g$. For the spherical confinement case, the calculation is performed in a cubic lattice with a 3-D spherical boundary (where diameter is d). The calculation started from random homogeneous initial mean fields $\omega_{A(B)}$. Under different surface fields, the spherical cavity diameter is varied to obtain systematic self-assembled structures of a bulk cylinder-forming diblock copolymer melt under spherical confinement.

Results and Discussion

The diblock copolymer chosen has a volume fraction of A-block $f_A = 0.2$ and a Flory−Huggins parameter $\chi N = 40$. This copolymer forms a hexagonally arranged cylindrical structure in the bulk.[43] From the bulk calculation, the polymer repeat period L is found to be $3.96R_g$. This block copolymer system is confined in a closed empty spherical cavity with diameter d, as shown in Figure 1. Under different surface fields, the self-assembled structures are displayed as a function of confinement dimension d/L. The results are summarized in Figure 2, where only the A-blocks are shown for clarity.

Neutral Surface ($H = 0$). The neutral surface case exhibits the influence of pure confinement on the equilibrium structures. As shown in the first row of Figure 2 ($H = 0$), the self-assembled

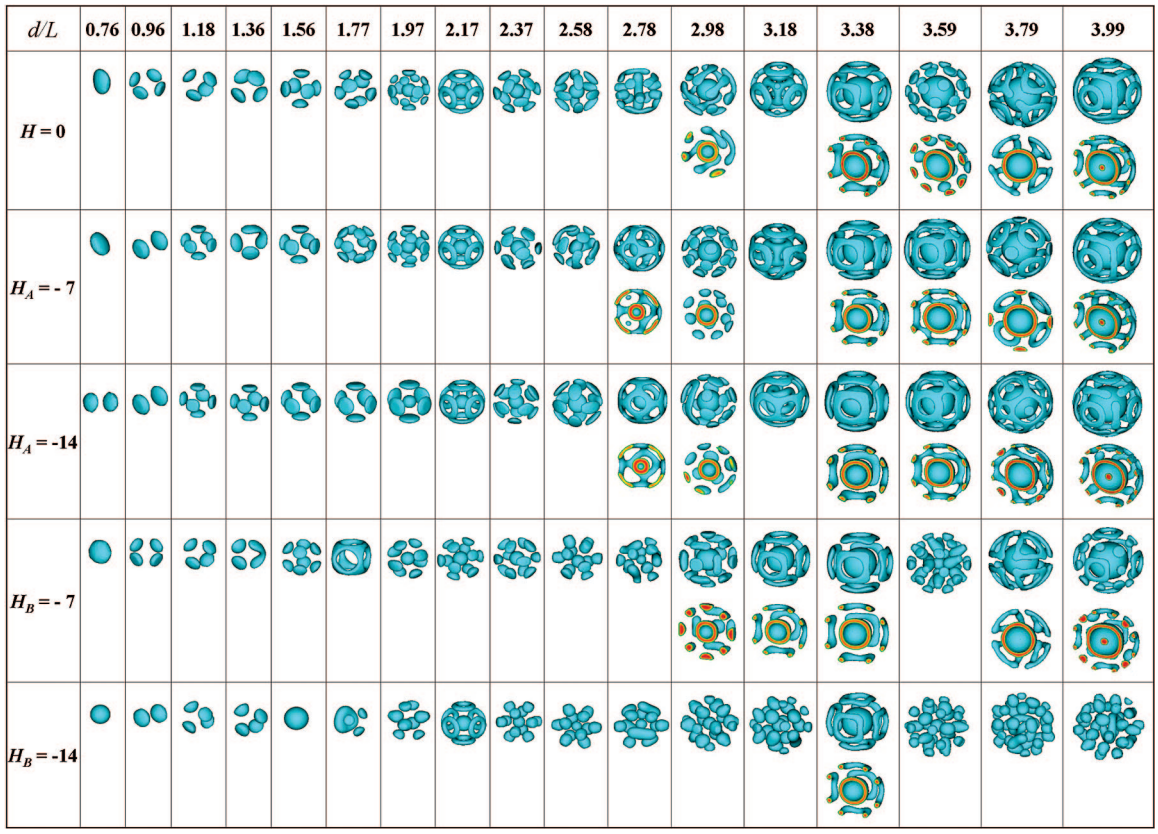

Figure 2. Spherical confinement induced microstructures of the cylinder-forming diblock copolymer under different surface fields (H) as a function of confinement dimension d/L (ratio of spherical cavity diameter d versus polymer repeat period L). Only A-blocks are shown, and some inner structures are shown under the full structures by cut views.

structures for this case are very complex. For convenience of description, the overall structures in Figure 2 are classified in terms of the number of A-monolayers (the monolayer structure formed by A-blocks), i.e., one layer ($d/L \leq 1.77$), two layers ($1.97 \leq d/L \leq 3.79$), and three layers ($d/L = 3.99$). It was noticed that the two- and three-layer structures started to form at around $d/L \approx 2.0$ and 4.0, that is, when the confinement diameter is an integer multiple of the polymer period.

As seen in the first row of Figure 2 for the neutral surface case, for small values of $d/L \leq 0.76$, an irregular A-block droplet is pasted on the inner surface of the confined spherical cavity. The remaining space is filled with B-blocks. With the confined space volume increasing to $d/L = 0.96$ (approximately 1.0), i.e., when the size of the confined space is near a polymer period, four small A-block droplets are found to be symmetrically arranged on the inner surface of the sphere. This symmetric structure evenly distributes the block copolymer chains in the confined space, maximizing the configurational entropy. With increasing d/L, the distribution and number of droplets are adjusted to fit in the confined space volume. Concurrently, the droplets maintain a well-ordered symmetric dispersion in the spherically confined space.

For the two-layer structures, the inner layer structures could be solid structures (such as a solid sphere or short cylinder) or empty structures (such as an empty sphere or perforated cubic). When $1.97 \leq d/L \leq 2.58$, the second A-monolayer, a solid sphere, forms in the center of the confined space. In most cases, the outside structures are evenly dispersed droplets ($d/L = 1.97$, 2.37, and 2.58), while at a suitable confinement diameter, such as $d/L = 2.17$, the outside layer is in the form of 6-fold symmetric circles. It was observed that at $d/L = 2.78$ a shorter cylinder, which is not a center-symmetric structure, forms surrounded by a number of droplets and stripes. Afterward, when

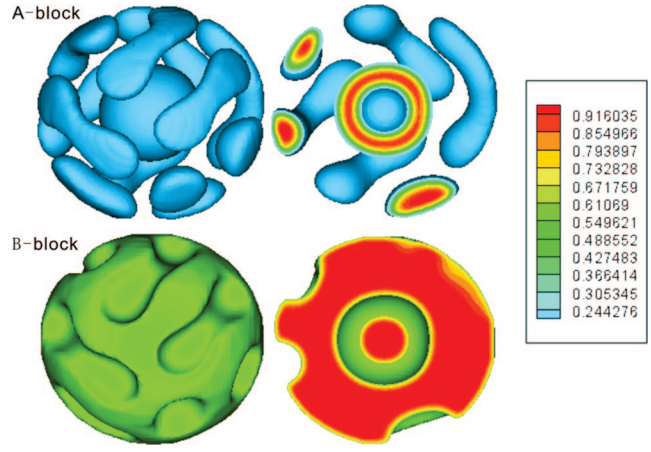

Figure 3. Inner empty sphere structure at $d/L = 2.98$, $H = 0$. The color bar shows the density values.

$2.98 \leq d/L \leq 3.79$, the inner A-monolayer structures become empty structures. The empty structure here means a B-rich domain in the center, separated (or partially separated) from the rest of the structure by a layer of A-blocks. Such as the inner empty sphere structure at $d/L = 2.98$, as Figure 3 shows, a B-block droplet in the center is covered by a A-block spherical cavity, in short an empty sphere. Such an empty sphere is prevalent in most inner layer structures, except at $d/L = 3.18$, which is a perforated cubic. As Figure 4 shows, the inner layer perforated cubic is strictly symmetric, which could be taken as a cubic evenly perforated in every direction. In Sevink's study, they also found perforated droplet structures.[44] Different from the perforated cubic structure, those structures are not cubic. With the large confinement space ($d/L \geq 2.98$), a larger number of stripes form on the outside layer. Such stripes may connect

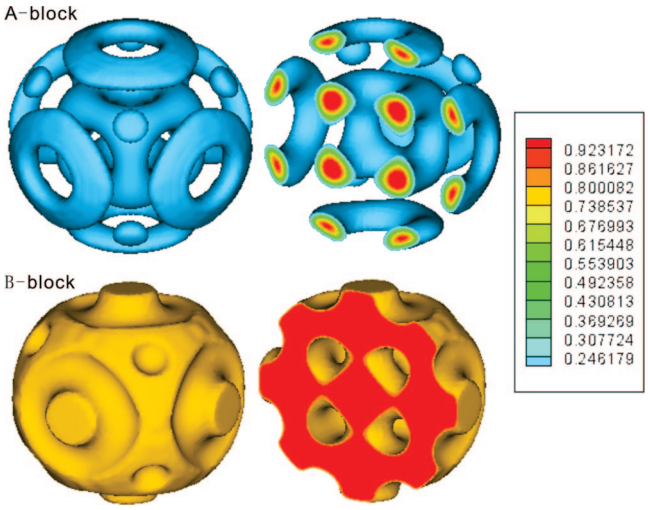

Figure 4. Inner layer perforated cubic structure at $d/L = 3.18$, $H = 0$. The color bar shows the density values.

into closed circles as d/L equals 3.38 and 3.79. In addition, the outside layer may still be dispersed droplets, as in the case of d/L at 3.59, or a complex of droplets with closed circles with $d/L = 3.18$. When $d/L = 3.99$, the third A-monolayer (inner layer), which is a solid sphere, forms in the confinement center, the second layer (intermediate layer) is an empty sphere, and the outside layer is a complex of six circles and a closed net. It seems that, under 3-D spherical confinement, outside structures of block copolymers are very arbitrary and are strongly dependent on the confined space volume, while inner structures robustly transit from solid sphere to empty sphere as the space volume increases. It can also be noted that the inner perforated cubic structure may appear under certain conditions (such as at $d/L = 3.18$).

In 2-D cylindrical confinement studies, the structure transition is well correlated with the confinement frustration. As the ratio of confinement diameter d versus polymer period L, d/L, changes from a half-integer to an integer, the structures turn from perpendicular cylinders to parallel cylinders.[29] In contrast, in the 3-D spherical confinement case, the structure transition is more or less arbitrary and the correlation with confinement frustration is weak. We consider that the reason for this is because 3-D confinement geometry produces more severe frustration on copolymer chains than those in 1-D or 2-D confinement. Spherical confinement prohibits the formation of long-range structures. At the same time, self-assembled structures in the spherical cavity possess a strong capacity to be center-symmetrical in order to fulfill entropy maximization of chain stretching. From the severe confinement effect and center-symmetrical confinement geometry, copolymers chains are forced to evenly disperse within the limited confined space, and gather into droplets, stripes, solid spheres, or empty spheres which vary from a bulk cylinder's structure.

A-Attractive Surface ($H_A < 0$). When the confinement surface attracts A-blocks, a behavior similar to that observed in the neutral surface cases is obtained. The confinement dimension d/L for the formation of similar multilayer structures is the same: one layer ($d/L \leq 1.77$), two layers ($1.97 \leq d/L \leq 3.79$), and three layers ($d/L = 3.99$), as shown in the second ($H_A = -7$) and third ($H_A = -14$) rows of Figure 2. The inner layer structures in A-attractive surface cases could also be a solid sphere, an empty sphere, or a perforated cubic, which are similar to those in neutral surface cases. The outside layer structures in A-attractive surface cases, owing to the surface preference effect, are always slightly varied from those in neutral surface cases.

However, as exhibited in some local details, the surface fields' effects on the equilibrium structure under 3-D spherical confinement are rather complicated. For example, at $d/L = 2.78$, the asymmetrical structure under a neutral surface field is reconstructed to be center-symmetrical under A-attractive surface fields. On the other hand, at $d/L = 3.18$, the center-symmetrical structure under a neutral surface field changed into asymmetrical ones under A-attractive surface fields. Furthermore, structures could remain unaffected under different surface fields, such as the structures at $d/L = 3.38$. Such inconsistent phenomena that the structures are unmovable or adjustable under different surface fields could be attributed to the effect of confinement on the self-assembly process. It is probably that in some severe frustration condition, wherein the equilibrium structure is highly strengthened; thus the surface field could hardly affect the self-assembled structure. Meanwhile, in some relaxed frustration condition, the equilibrium structure is easily reconstructed by the surface field; as a result, the copolymer chains could adjust themselves to adapt to the surface preference.

Until now, the detailed analysis of the 3-D confinement effect on the structure formation remains to be determined. As Sevink et al. demonstrated in the study of block copolymers confined in a nanopore,[33] there are several factors acting, both kinetic and thermodynamic, on the polymer self-assembly in the curving and frustrating flatland. Further study to determine the structure formation under spherical confinement should combine the kinetic and thermodynamic data.

B-Attractive Surface ($H_B < 0$). Studies on diblock copolymer self-assembly under 2-D cylindrical confinement[28,29] revealed that cylinder-forming diblock copolymers systems experience similar phase behaviors in all kinds of surface field cases, indicating that self-assembled structures under an A-attractive surface field also form under a B-attractive surface field or a neutral surface field. Contrary to this phenomenon, this research discovered that in spherical confinement self-assembled structures under a B-attractive surface field are different from those under neutral and A-attractive surface fields.

For the weak B-attractive surface case ($H_B = -7$) seen in the fourth row of Figure 2, the A-blocks are repelled from the surface in comparison to the neutral surface and A-attractive surface cases. When the confined space is small ($0.76 \leq d/L \leq 1.56$), either droplets form or a complex of droplets with stripes ($d/L = 1.36$) appears. A perforated cubic structure arises at $d/L = 1.77$, similar to the inner perforated cubic structures at $d/L = 3.18$ under neutral ($H = 0$) and weak A-attractive surface field ($H_A = -7$) cases. Moreover, it resides between the regions for one-layer and two-layer structures. When $1.97 \leq d/L \leq 2.78$, two-layer structures mainly composed by droplets are formed. With an increase in confinement diameter, that is, when $2.98 \leq d/L \leq 3.79$, most inner layer structures become empty spheres, just like the ones in the neutral and A-attractive surface cases. However, at a certain condition, such as $d/L = 3.59$, a structure totally composed of droplets is formed. In neutral and A-attractive surface field cases, when the confinement diameter is large enough for inner empty sphere structures to form, no structure composed mainly of droplets appears. The formation of droplet structure at $d/L = 3.59$ (B-attractive surface cases) indicates that the phase behavior of block copolymer under a B-attractive surface field is different from those under neutral and A-attractive surface fields.

A close inspection of the self-assembled structures under a strong B-attractive surface field ($H_B = -14$) in the fifth row of Figure 2 provides a clearer impression of the unique phase behavior of block copolymers under B-attractive surface fields. At $d/L = 1.56$, it forms a solid sphere in the center of spherical confinement, which, in spite of the smaller space ($0.96 \leq d/L \leq 1.36$) and larger space ($d/L \geq 1.77$), are both apt for the

separated structures. As it is different from the neutral and A-attractive surface cases, and even the weak B-attractive surface case ($H_B = -7$), when $d/L \geq 2.78$, the inner empty sphere structure is very seldom formed in a strong B-attractive surface case ($H_B = -14$). Only at $d/L = 3.38$ for the strong B-attractive surface case ($H_B = -14$) does the inner empty sphere and six symmetrical circle structure outside retain the same as that of all other surface fields cases ($H = 0$, $H_A = -7$, $H_A = -14$, and $H_B = -7$). The structures of the complex of droplets are prevalent in a strong B-attractive surface case ($H_B = -14$). Even at greater confinement diameters, such as $3.79 \leq d/L \leq 3.99$, the structures are the complex of outside droplets and inner distorted cylinders.

As asserted above, in 3-D spherical confinement, self-assembled structures under B-attractive surface fields are clearly different from those under neutral and A-attractive surface fields, especially for equilibrium structures under strong B-attractive surface fields. Such a phenomenon is not consistent with that in 2-D cylindrical confinement. Under 2-D cylindrical confinement,[28,29] studies indicate that outside layer structures could screen out the surface field; hence, inner layer structures are less affected by the surface field. As a result, the equilibrium structures, except for those in the outside layer, are similar to those under all kinds of surface fields. This research attributes the difference between 2-D cylindrical confinement and 3-D spherical confinement to two factors. First, the surface field under 3-D spherical confinement which rises in all directions thus causes the block copolymer's phase behavior to suffer more from the surface field. Second, the 3-D spherical confinement geometry causes the inner layer polymers to experience more severe frustration than the inner layer polymers do in 2-D confinement.

Structure Transition with *d/L* Increasing. Within the scope of this study, the general trend of structural transition is from one layer to several layers. We number the structure layers by counting the separated A-block domain as n. It is easily assumed that the value of n must have a maximum because the confined system would act like a bulk one when the confinement geometry gets large enough. Limited by computer capability, however, the value of n could not be asserted. From Figure 2, we found that the structures' transition points for increasing layers have the following expression: $d/L \approx 2(n - 1)$. For $n = 2$, $d/L \approx 2$; for $n = 3$, $d/L \approx 4$. In ref 38, when a symmetric diblock copolymer is confined in a spherical state, the expression $d/L \approx 2(n - 1)$ seems to fit the case of strong surface-preference limit. For the A-block domain, the two-layer structure started at $d/L = 2$, while the three-layer started at $d/L = 4.2$ ($a \approx 1$ in Figure 1a, ref 38).

The expression could be changed to $n \approx 1/2(d/L) + 1$. According to this, in the spherical confinement state, the experimental research can control the number of structural layers by setting the confinement geometry dimensions.

Comparison with Experimental and Simulation Observations. To this date, few experiments have concentrated on asymmetric diblock copolymer self-assembly under 3-D spherical confinement. The study by Thomas's team on a bulk cylinder polymer system in a microdrop indicates that there are several layers of curved concentric arrays formed.[35] However, in our research, the cut view (in ref 35, Figure 12-C) may arise from several conditions, such as a mixture of droplet structures (i.e., $d/L = 3.59$ in $H_B = -7$ and -14) or the complex of outside stripes, middle empty sphere, and inner solid sphere structures (i.e., $d/L = 3.99$ in $H = 0$, $H_A = -7$, $H_A = -14$, and $H_B = -7$).

In Feng et al.'s dissipative particle dynamics (DPD) approach on the self-assembly of asymmetric A_3B_7 and A_2B_8 diblock copolymers, they discovered bended sticks and polygon structures.[39] Such structures are less regular, partially because the DPD study of Feng et al. is dynamic, as kinetic trapping is known to easily happen in the dynamic process. However, the transition from monolayer to multilayer structures is consistent with the observations in this study. Moreover, the spheres or peanut-like structures in their study are comparable with the complex structure of droplets in this work.

Conclusions

In conclusion, the self-assembly of cylinder-forming diblock copolymers under 3-D spherical confinement can produce more complex and fundamentally different structures from bulk cylinders. These structures could not be produced in bulk or other 1-D or 2-D confinement geometries. The self-assembled structures under B-attractive surface fields are clearly different from those observed under neutral and A-attractive surface fields. It is demonstrated that the self-assembly of asymmetric diblock copolymers under 3-D spherical confinement is rather complicated, and in some cases, the self-assembled structure is arbitrary and the transition sequence is difficult to identify. The calculation results in this study should be instructive for the experimental research and subsequent theoretical exploration in related fields.

Acknowledgment. The authors are grateful for the financial support provided by the Outstanding Youth Fund (No. 20525416), the Programs of the National Natural Science Foundation of China (Nos. 20490220 and 90403022), and the National Basic Research Program of China (No. 2005CB623800). ACS is supported by the Natural Sciences and Engineering Council (NSERC) of Canada. Parts of the calculations were carried out at the Shanghai Supercomputer Center.

Supporting Information Available: Spherical confinement induced microstructures of the cylinder-forming diblock copolymer under different surface fields (H, H_A, and H_B), inner empty sphere structures, and inner layer perforated structures, as a function of confinement dimensions d/L. This material is available free of charge via the Internet at http://pubs.acs.org.

References and Notes

(1) Bates, F. S.; Fredrickson, G. H. *Annu. Rev. Phys. Chem.* **1990**, *41*, 525.
(2) Park, M.; Harrison, C.; Chaikin, P. M.; Register, R. A.; Adamson, D. H. *Science* **1997**, *276*, 1401.
(3) Bates, F. S.; Fredrickson, G. H. *Phys. Today* **1999**, *52*, 32.
(4) Pereira, G. G. *Curr. Appl. Phys.* **2004**, *4*, 255.
(5) Grason, G. M. *Phys. Rep.* **2006**, *433*, 1.
(6) He, X. H.; Song, M.; Liang, H. J.; Pan, C. Y. *J. Chem. Phys.* **2001**, *114*, 10510.
(7) Sevink, G. J. A.; Zvelindovsky, A. V.; Fraaije, J.; Huinink, H. P. *J. Chem. Phys.* **2001**, *115*, 8226.
(8) Knoll, A.; Horvat, A.; Lyakhova, K. S.; Krausch, G.; Sevink, G. J. A.; Zvelindovsky, A. V.; Magerle, R. *Phys. Rev. Lett.* **2002**, *89*, 035501.
(9) Ludwigs, S.; Boker, A.; Voronov, A.; Rehse, N.; Magerle, R.; Krausch, G. *Nat. Mater.* **2003**, *2*, 744.
(10) Park, I.; Park, S.; Park, H. W.; Chang, T.; Yang, H. C.; Ryu, C. Y. *Macromolecules* **2006**, *39*, 315.
(11) Matsen, M. W. *J. Chem. Phys.* **1997**, *106*, 7781.
(12) Huinink, H. P.; Brokken-Zijp, J. C. M.; van Dijk, M. A.; Sevink, G. J. A. *J. Chem. Phys.* **2000**, *112*, 2452.
(13) Huinink, H. P.; van Dijk, M. A.; Brokken-Zijp, J. C. M.; Sevink, G. J. A. *Macromolecules* **2001**, *34*, 5325.
(14) Wang, Q.; Nealey, P. F.; de Pablo, J. J. *Macromolecules* **2001**, *34*, 3458.
(15) Xu, T.; Hawker, C. J.; Russell, T. P. *Macromolecules* **2005**, *38*, 2802.
(16) Ludwigs, S.; Schmidt, K.; Stafford, C. M.; Amis, E. J.; Fasolka, M. J.; Karim, A.; Magerle, R.; Krausch, G. *Macromolecules* **2005**, *38*, 1850.
(17) Ludwigs, S.; Krausch, G.; Magerle, R.; Zvelindovsky, A. V.; Sevink, G. J. A. *Macromolecules* **2005**, *38*, 1859.
(18) Chen, P.; Liang, H. *J. Phys. Chem. B* **2006**, *110*, 18212.
(19) Xiang, H.; Shin, K.; Kim, T.; Moon, S. I.; McCarthy, T. J.; Russell, T. P. *Macromolecules* **2004**, *37*, 5660.

(20) Sun, Y. M.; Steinhart, M.; Zschech, D.; Adhikari, R.; Michler, G. H.; Gosele, U. *Macromol. Rapid Commun.* **2005**, *26*, 369.
(21) Xiang, H.; Shin, K.; Kim, T.; Moon, S. I.; McCarthy, T. J.; Russell, T. P. *Macromolecules* **2005**, *38*, 1055.
(22) Chen, P.; He, X. H.; Liang, H. J. *J. Chem. Phys.* **2006**, *124*, 104906.
(23) Feng, J.; Ruckenstein, E. *Macromolecules* **2006**, *39*, 4899.
(24) Wang, Q. *J. Chem. Phys.* **2007**, *126*, 024903.
(25) Wu, Y. Y.; Cheng, G. S.; Katsov, K.; Sides, S. W.; Wang, J. F.; Tang, J.; Fredrickson, G. H.; Moskovits, M.; Stucky, G. D. *Nat. Mater.* **2004**, *3*, 816.
(26) Shin, K.; Xiang, H. Q.; Moon, S. I.; Kim, T.; McCarthy, T. J.; Russell, T. P. *Science* **2004**, *306*, 76.
(27) Xiang, H.; Shin, K.; Kim, T.; Moon, S.; McCarthy, T. J.; Russell, T. P. *J. Polym. Sci., Part B: Polym. Phys.* **2005**, *43*, 3377.
(28) Li, W.; Wickham, R. A. *Macromolecules* **2006**, *39*, 8492.
(29) Yu, B.; Sun, P. C.; Chen, T. C.; Jin, Q. H.; Ding, D. T.; Li, B. H.; Shi, A. C. *Phys. Rev. Lett.* **2006**, *96*, 138306.
(30) Feng, J.; Ruckenstein, E. *J. Chem. Phys.* **2006**, *125*, 164911.
(31) Yu, B.; Sun, P.; Chen, T.; Jin, Q.; Ding, D.; Li, B.; Shi, A.-C. *J. Chem. Phys.* **2007**, *126*, 204903.
(32) Chen, P.; Liang, H.; Shi, A. C. *Macromolecules* **2007**, *40*, 7329.
(33) Sevink, G. J. A.; Zvelindovsky, A. V. *J. Chem. Phys.* **2008**, *128*, 084901.
(34) Li, W. H.; Wickham, R. A.; Garbary, R. A. *Macromolecules* **2006**, *39*, 806.
(35) Cheng, J. Y.; Ross, C. A.; Smith, H. I.; Thomas, E. L. *Adv. Mater.* **2006**, *18*, 2505.
(36) Arsenault, A. C.; Rider, D. A.; Tetreault, N.; Chen, J. I. L.; Coombs, N.; Ozin, G. A.; Manners, I. *J. Am. Chem. Soc.* **2005**, *127*, 9954.
(37) Fraaije, J. G. E. M.; Sevink, G. J. A. *Macromolecules* **2003**, *36*, 7891.
(38) Yu, B.; Li, B. H.; Jin, Q. H.; Ding, D. T.; Shi, A. C. *Macromolecules* **2007**, *40*, 9133.
(39) Feng, J.; Liu, H.; Hu, Y. *Fluid Phase Equilib.* **2007**, *261*, 50.
(40) Drolet, F.; Fredrickson, G. H. *Phys. Rev. Lett.* **1999**, *83*, 4317.
(41) Drolet, F.; Fredrickson, G. H. *Macromolecules* **2001**, *34*, 5317.
(42) Chen, H. Y.; Fredrickson, G. H. *J. Chem. Phys.* **2002**, *116*, 1137.
(43) Matsen, M. W.; Bates, F. S. *Macromolecules* **1996**, *29*, 1091.
(44) Sevink, G. J. A.; Zvelindovsky, A. V. *Mol. Simul.* **2007**, *33*, 405.

MA800443H